

## Gold-Catalyzed Cycloisomerization of 1,5-Allenynes via Dual Activation of an Ene Reaction

Paul Ha-Yeong Cheong,<sup>†</sup> Philip Morganelli,<sup>‡</sup> Michael R. Luzung,<sup>‡</sup> K. N. Houk,<sup>\*,†</sup> and F. Dean Toste<sup>\*,‡</sup>

Department of Chemistry, University of California, Berkeley, California 94720, and Department of Chemistry and Biochemistry, University of California, Los Angeles, California 90095-1569

Received December 12, 2007; E-mail: houk@chem.ucla.edu; fdtoste@berkeley.edu

**Abstract:** Tris(triphenylphosphinegold) oxonium tetrafluoroborate, [(Ph<sub>3</sub>PAu)<sub>3</sub>O]BF<sub>4</sub>, catalyzes the rearrangement of 1,5-allenynes to produce cross-conjugated trienes. Experimental and computational evidence shows that the ene reaction proceeds through a unique nucleophilic addition of an allene double bond to a cationic phosphinegold(I)-complexed phosphinegold(I) acetylide, followed by a 1,5-hydrogen shift.

### Introduction

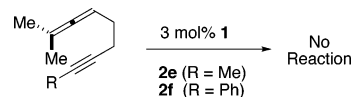
Transition metal-catalyzed allenyne cycloisomerization reactions provide an atom-economical entry into polyunsaturated carbo- and heterocycles.<sup>1–3</sup> These reactions involving Rh, Pd, or Pt are generally postulated to proceed via metallacyclopentene intermediates, inherently involving an increase in the formal oxidation state of the metal.<sup>1,4</sup> On the other hand, gold(I)-catalyzed enyne<sup>5</sup> and some related 1,6-allenyne cycloisomerization reactions<sup>6</sup> are proposed to proceed without a change in the formal oxidation state of the catalyst.<sup>7</sup> We report a combined experimental and computational investigation of gold(I) catalysis of an allenyne cyclization that proceeds via a unique mechanism involving cationic phosphinegold(I) activation of an in situ generated phosphinegold(I) acetylide.<sup>2,8–10</sup>

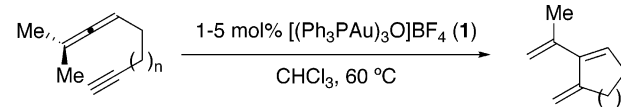
**Substrate Scope.** Reaction of 1,5-allenyne **2a** under typical conditions for the cycloisomerization of 1,5-enynes [1 mol % Ph<sub>3</sub>PAuCl, 1 mol % AgSbF<sub>6</sub>, CH<sub>2</sub>Cl<sub>2</sub>, room temperature (rt)]<sup>5c</sup> resulted in rapid formation of a complex mixture. Switching the catalyst to the less reactive tris(phosphinegold)oxonium complex [(Ph<sub>3</sub>PAu)<sub>3</sub>O]BF<sub>4</sub> **1** furnished triene **3a** in 31% yield. The yield was further improved to 88% when the reaction was conducted at 60 °C in chloroform (Table 1, entry 1). Under these optimal conditions, a variety of 1,5-allenynes participate in the gold-catalyzed cycloisomerization. Substitutions on the tether (entries 1–6) and on the allene moiety (entries 7 and 8) are well tolerated.<sup>11</sup> Both diastereomers of bicyclo[4.3.0]nonanes **5a,b** could be prepared with complete retention of stereochemistry. In addition to cyclopentenes, cyclohexene **11** was produced from the gold-catalyzed cycloisomerization of 1,6-allenyne **10**, albeit with diminished yield (entry 9). Of mechanistic importance, nonterminal alkyne substrates were inert under these conditions.<sup>12,13</sup>

<sup>†</sup> University of California, Los Angeles.

<sup>‡</sup> University of California, Berkeley.

- Allenyne cycloisomerizations proceeding through metallacyclopentene intermediates: For Rh, (a) Brummond, K. M.; Chen, H.; Sill, P.; You, L. *J. Am. Chem. Soc.* **2002**, *124*, 15186. (b) Shibata, T.; Takesue, Y.; Kadowaki, S.; Takagi, K. *Synlett* **2003**, 268. (c) Mukai, C.; Inagaki, F.; Yoshida, T.; Kitagaki, S. *Tetrahedron Lett.* **2004**, *45*, 4117. For Ti, (d) Urabe, H.; Takeda, T.; Hideura, D.; Sato, F. *J. Am. Chem. Soc.* **1997**, *119*, 11295. For Pt, (e) Cadran, N.; Cariou, K.; Herve, G.; Aubert, C.; Fensterbank, L.; Malacria, M.; Marco-Contelles, J. *J. Am. Chem. Soc.* **2004**, *126*, 3408. (f) Matsuda, T.; Kadowski, S.; Goyam, T.; Murakami, M. *Synlett* **2006**, 575. For Mo, (g) Shen, Q.; Hammond, G. B. *J. Am. Chem. Soc.* **2002**, *124*, 6534.
- Alternative mechanisms for allenyne cycloisomerization: For Co, (a) Lierena, D.; Aubert, C.; Malacria, M. *Tetrahedron Lett.* **1996**, *37*, 7027. For Ga, (b) Lee, S. I.; Sim, S. H.; Kim, S. M.; Kim, K.; Chung, Y. K. *J. Org. Chem.* **2006**, *71*, 7120. For Mo-catalyzed allenyne metathesis, (c) Murakami, M.; Kadowski, S.; Matsuda, T. *Org. Lett.* **2005**, *7*, 3953.
- Thermal reactions of allenynes: (a) Ohno, H.; Mizutani, T.; Kadoh, Y.; Miyamura, K.; Tanaka, T. *Angew. Chem., Int. Ed.* **2005**, *44*, 5113. (b) Oh, C. H.; Gupta, A. K.; Park, D. I.; Kim, N. *Chem. Commun.* **2005**, 5670.
- DFT-based theoretical study of the Pt(II)-catalyzed cycloisomerization of allenynes: Soriano, E.; Marco-Contelles, J. *Chem – Eur. J.* **2005**, *11*, 521.
- Cycloisomerization of 1,5- and 1,6-enynes involving nucleophilic addition of olefins to gold(I)-acetylene complexes: (a) Nieto-Oberhuber, C.; Muñoz, M. P.; Buñuel, E.; Nevado, C.; Cárdenas, D. J.; Echavarren, A. M. *Angew. Chem., Int. Ed.* **2004**, *43*, 2402. (b) Mamane, V.; Gress, T.; Krause, H.; Fürstner, A. *J. Am. Chem. Soc.* **2004**, *126*, 8654. (c) Luzung, M. R.; Markham, J. P.; Toste, F. D. *J. Am. Chem. Soc.* **2004**, *126*, 10858. (d) Nieto-Oberhuber, C.; López, S.; Echavarren, A. M. *J. Am. Chem. Soc.* **2005**, *127*, 6178. (e) Gagosz, F. *Org. Lett.* **2005**, *7*, 4129. (f) Sun, J.; Conley, M. P.; Zhang, L.; Kozmin, S. A. *J. Am. Chem. Soc.* **2006**, *128*, 9705. (g) Fehr, C.; Galindo, J. *Angew. Chem., Int. Ed.* **2006**, *45*, 2901. (h) Park, S.; Lee, D. *J. Am. Chem. Soc.* **2006**, *128*, 10664. (i) Horino, Y.; Luzung, M. R.; Toste, F. D. *J. Am. Chem. Soc.* **2006**, *128*, 11364. For reviews: (i) Nieto-Oberhuber, C.; López, A.; Jiménez-Núñez, E.; Echavarren, A. M. *Chem. Eur. J.* **2006**, *12*, 5916. (j) Ma, S.; Yu, S.; Gu, Z. *Angew. Chem., Int. Ed.* **2006**, *45*, 200.
- (a) Lemièrre, G.; Gandon, V.; Agenet, N.; Goddard, J.-P.; de Kozak, A.; Aubert, C.; Fensterbank, L.; Malacria, M. *Angew. Chem., Int. Ed.* **2006**, *45*, 7596. (b) The allyl cation intermediate was trapped by the use of deuterated methanol. (c) Protodemetalations are known to occur stereoselectively. In the case of 1,6-allenyne rearrangements, the same anti incorporation of deuterium was observed.
- Recent reviews of gold-catalyzed reactions: (a) Jiménez-Núñez, E.; Echavarren, A. M. *Chem. Commun.* **2007**, 333. (b) Gorin, D. J.; Toste, F. D. *Nature* **2007**, *446*, 395. (c) Fürstner, A.; Davies, P. W. *Angew. Chem., Int. Ed.* **2007**, *46*, 2. (d) Hashmi, A. S. K. *Chem. Rev.* **2007**, *107*, 3180.
- Gupta, A. K.; Rhim, C. Y.; Oh, C. H.; Mane, R. S.; Han, S.-H. *Green Chem.* **2006**, *8*, 25.
- Dipolar cycloadditions catalyzed by a two copper mechanism have been reported recently: Ahlquist, M.; Fokin, V. V. *Organometallics* **2007**, *26*, 4389.
- A related allenyne rearrangement has been reported: Zriba, R.; Gandon, V.; Aubert, C.; Fensterbank, L.; Malacria, M. *Chem.–Eur. J.* **2008**, *14*, 1482.
- A preference for formation of **Z-9a** can be rationalized by conformational analysis of the proton transfer step. A conformation leading to an *E*-olefin, placing ethyl planar with phenyl group, introduces a significant strain. The final product distribution of 7:1, corresponding to an energy difference of 1.2 kcal/mol, is an acceptable value for A(1,2)-strain.
- Both alkyl- (**2e**) and aryl- (**2f**) substituted alkynes failed to react under the reported reactions conditions. See Experimental Section for details.

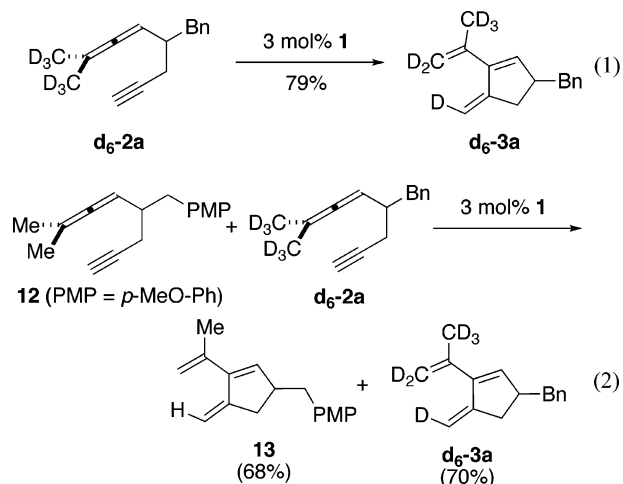


**Table 1.** Scope of Gold(I)-Catalyzed Allenyne Cycloisomerization


| entry          | substrate | mol% 1 | product(s) | yield <sup>a</sup>                                  |
|----------------|-----------|--------|------------|---|
| 1              |           | 5      |            | <b>3a</b> 88%                                       |
| 2              |           | 2      |            | <b>b</b> 84%  |
| 3 <sup>b</sup> |           | 2      |            | <b>c</b> 89%  |
| 4 <sup>b</sup> |           | 2      |            | <b>d</b> 99%  |
| 5              |           | 1      |            | <b>5a</b> 78%                                       |
| 6              |           | 1      |            | <b>b</b> 70%  |
| 7              |           | 3      |            | <b>7</b> 70%  |
| 8 <sup>c</sup> |           | 3      |            | 64%<br>2.4:1<br><b>9a</b><br>(7:1 Z:E)<br><b>9b</b> |
| 9              |           | 5      |            | <b>11</b> 40%                                       |

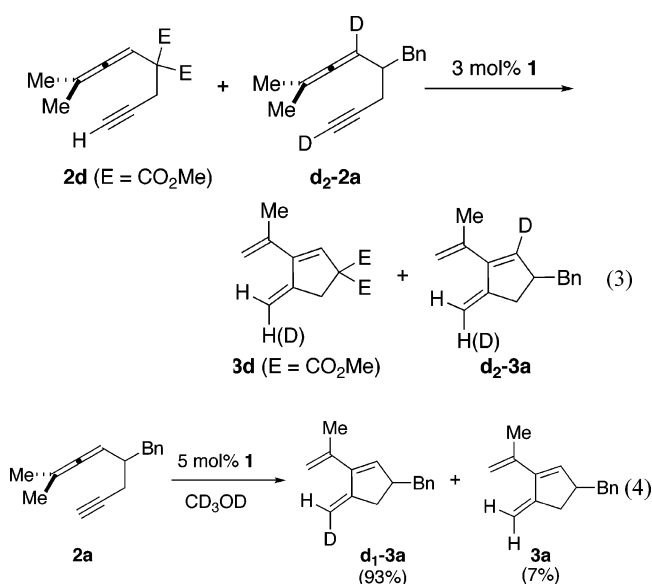
<sup>a</sup> Isolated yields after flash column chromatography. For reaction times, see Supporting Information. <sup>b</sup> Reaction was run in CH<sub>2</sub>Cl<sub>2</sub> at 40 °C. <sup>c</sup> Regio- and stereoselectivities measured by <sup>1</sup>H NMR.

**Deuterium Labeling Experiments.** Deuterium labeling experiments reveal that the hydrogen transfer is stereoselective; the allenic hydrogen is always incorporated syn to the newly formed C–C bond (eq 1). A double-labeled crossover



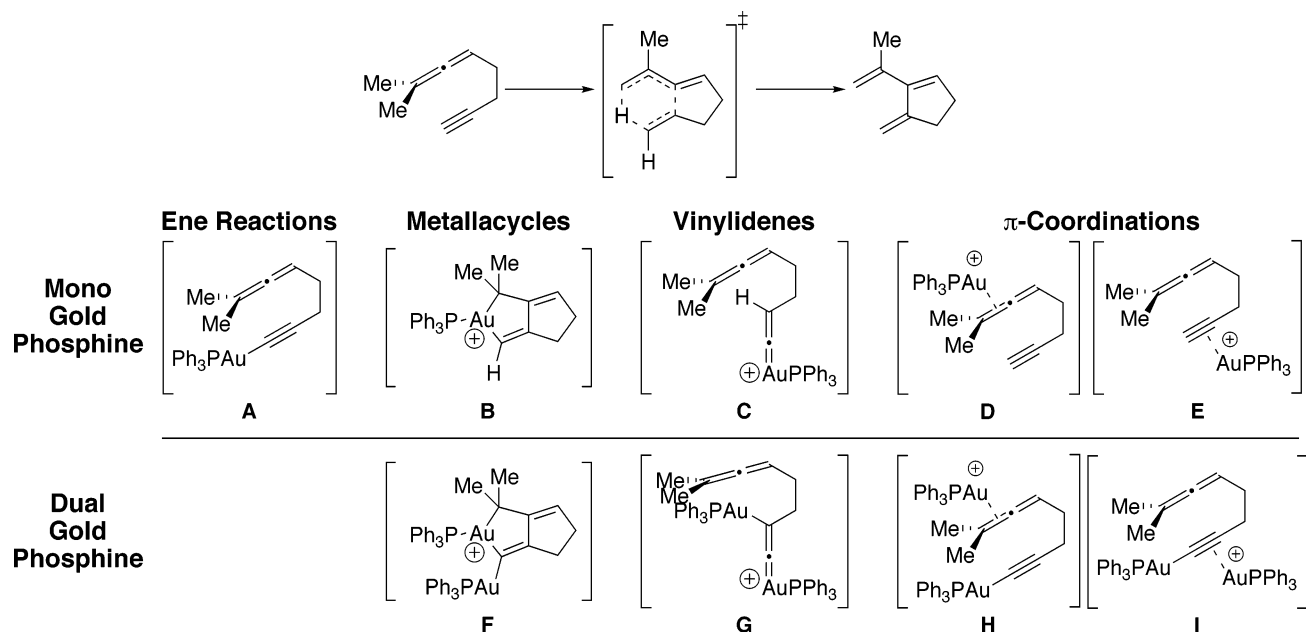
experiment showed no exchange of the deuterium label, suggesting the reaction proceeds through an intramolecular

hydrogen transfer (eq 2). The proton at the alkyne terminus, however, does exchange (eq 3). In deuterated methanol, nearly complete anti incorporation of deuterium is observed in the product (eq 4).

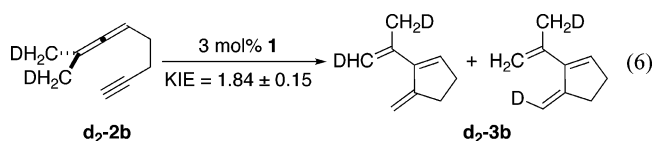
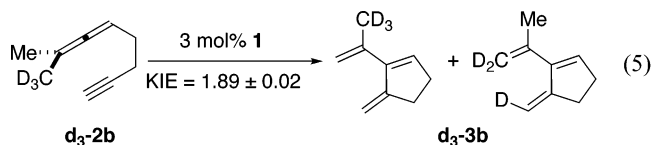


(13) In contrast, triphenylphosphine hexafluoroantimonate catalyzed the cycloisomerization of 1,6-allenynes containing phenyl-substituted alkynes via a tandem 5-endo-dig/Nazarov cyclization mechanism: Lin, G.-Y.; Yang, C.-Y.; Liu, R. S. *J. Org. Chem.* **2007**, *72*, 6753. Related 6-endo-dig cyclization of allenynes: Zhao, J.; Hughes, C. O.; Toste, F. D. *J. Am. Chem. Soc.* **2006**, *128*, 7436.

**Kinetic Isotope Effect.** Two kinetic isotope experiments were performed (eqs 5 and 6). The  $k_{\text{CD}_3}/k_{\text{CH}_3}$  isotope effect ( $1.89 \pm 0.02$ ) and the  $k_{\text{H}}/k_{\text{D}}$  isotope effect ( $1.84 \pm 0.15$ ) were essentially

**Scheme 1.** Potential Intermediates Involved in the Trimer (1)-Catalyzed Allene Cycloisomerization

identical, suggesting that the formal 1,5-sigmatropic shift is responsible for the measured isotope effects. Additionally, these measured kinetic isotope effects are much smaller than the typical values of 3–5 for 1,5-sigmatropic shifts.<sup>14–16</sup>



**Proposed Mechanisms.** Numerous mechanistic possibilities exist for catalysis of this formal ene reaction (top, Scheme 1). In fact, no less than nine possibilities emerged during our investigation.

The mechanism through **B** involves an oxidative cyclization of the allenyne to form gold(III)-metallacycle, followed by  $\beta$ -hydride elimination and reductive elimination. Mechanisms involving **A** and **C** are ene reactions of phosphinegold vinylidene and phosphinegold acetylide, respectively. Mechanisms through **D** and **E** are ene reactions catalyzed by the coordination of a phosphinegold to either the acetylene or allene<sup>17</sup> in the substrate. Mechanisms **F–I** are transformations analogous to **B–E** involving a phosphinegold acetylide.

A mechanism involving double activation by phosphinegold (**I**) is plausible. This is supported by three experimental observations: (i) inertness of nonterminal alkyne substrates under reaction conditions,<sup>12</sup> (ii) deuterium exchange at the terminal alkyne position (eq 4), and (iii) observation of the transient formation of phosphinegold acetylide **2a'** from **2a** under the reaction conditions.<sup>18</sup> We believe this reaction to undergo catalysis via species **I**.<sup>19</sup>

**Computational Method.** The geometry optimizations and thermodynamic corrections were performed with hybrid density functional theory (B3LYP) with the 6-31+G\* and LANL2DZ+ECP basis sets. Solvation corrections for chloroform were computed by the PCM method with single points at the HF level with 6-31+G(d,p) and LANL2DZ basis sets. All calculations were performed with the Gaussian series of programs.<sup>20</sup>

The computationally investigated reaction was the conversion of unsubstituted substrate **2b** to triene product **3b**. Phosphine was used as a model for the triphenylphosphine. Species involving the triphenylphosphine were also optimized to compare experimental and computed kinetic isotope effects (KIEs). Computed KIEs between transition structures involving simple phosphines and triphenyl phosphines were indistinguishable in all computed cases.

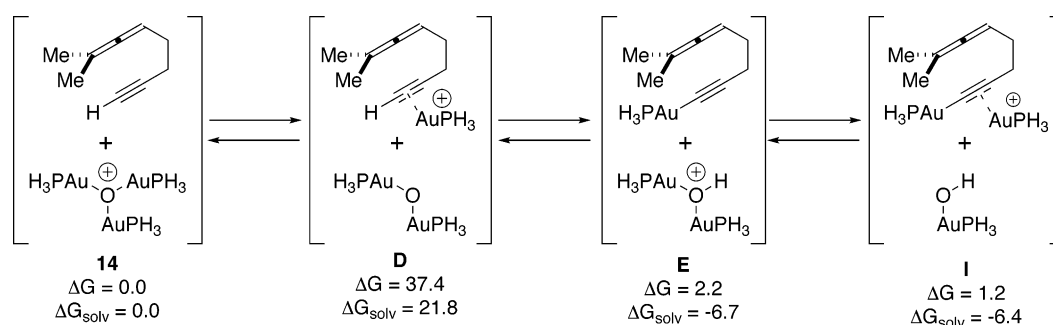
All relative energies presented in this paper are free energies in kilocalories per mole, with respect to separated substrate and tris(phosphinegold)oxonium catalyst complex.

**Possible Substrate–Gold Complexes.** The tris[phosphinegold(I)]oxonium catalyst **1** can transfer a phosphinegold cation

(14) Houk, K. N.; Li, Y.; Evanseck, J. D. *Angew. Chem., Int. Ed.* **2003**, *31*, 682.  
 (15) Examples: Doering, W. von E.; Zhao, X. *J. Am. Chem. Soc.* **2006**, *126*, 9080 and references therein.  
 (16) A  $k_{CD_3}/k_{CH_3}$  isotope effect of 1.43 was measured in the related Schmitt-ene cyclization of enyne-allenes: Bekele, T.; Christian, C. F.; Lipton, M. A.; Singleton, D. A. *J. Am. Chem. Soc.* **2005**, *127*, 9216.  
 (17) Coordination of cationic triphenylphosphinegold(I) to the internal olefin of the allene does not lead to viable catalysis and therefore was excluded from analyses.

(18) The <sup>1</sup>H NMR spectrum of acetylide **2a'** was compared to the spectrum obtained from a reaction in progress of **2a** with stoichiometric quantities of trimer **1**. A transient peak at 5.05 ppm observed in the latter spectrum is a match with the C<sub>5</sub> proton of the acetylide spectrum at 5.07 ppm.  
 (19) A related dual-activation mechanism has recently been proposed for the copper-catalyzed azide-alkyne cycloaddition: Ahlquist, M.; Fokin, V. V. *Organometallics* **2007**, *26*, 4389.  
 (20) Frisch, M. J.; et al. *Gaussian 03*, Revision C.02; Gaussian, Inc.: Pittsburgh, PA, 2004.

Scheme 2. Possible Substrate–Gold Complexes



to the alkyne, a process with an unfavorable enthalpy and entropy ( $\Delta G = 37.4$  and  $\Delta G_{\text{solv}} = 21.8$  kcal/mol, **E**), although this is likely to be much more favorable with sterically hindered phosphines. The formation of phosphinegold acetylide is very favorable, and subsequent transfer of a second phosphinegold cation is also favorable (Scheme 2).

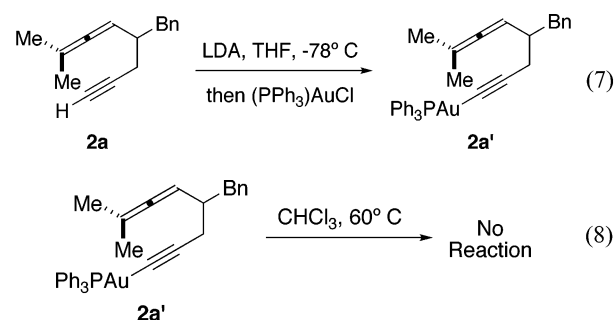
**Uncatalyzed Reaction: Ene Reaction of 1,5-Allenynes.** The parent uncatalyzed ene reaction involves a concerted C–C bond formation and asynchronous hydrogen transfer (Figure 1). The free energy barrier of this process ( $\Delta G^\ddagger = 33.0$  and  $\Delta G_{\text{solv}}^\ddagger = 32.3$  kcal/mol, **TS-15**) is typical for pericyclic reactions.<sup>17</sup> The reaction exergonicity is computed to be large ( $\Delta G_{\text{rxn}} = \sim -38$  kcal/mol, **16**).

**Mechanism via A: Ene Reaction of Phosphinegold Acetylide.** The ene reaction of phosphinegold acetylide, **A**, was postulated by analogy to copper-catalyzed pericyclic reactions.<sup>22</sup> The coordination of copper(I) to a terminal alkyne reportedly lowers the  $pK_a$  of the proton by  $\sim 8$   $pK_a$  units, allowing for facile formation of copper acetylides.<sup>22</sup> A similar pathway is proposed for the formation of phosphinegold acetylide (see Scheme 2).

Computationally, the ene reaction via **A** is found to be extremely similar to the uncatalyzed reaction; it features concerted C–C bond formation and highly asynchronous hydrogen transfer (**A-TS-1** in Figure 2). The computed free energy barrier ( $\Delta G^\ddagger = 35.2$  and  $\Delta G_{\text{solv}}^\ddagger = 34.0$  kcal/mol) is approximately equal to that of the uncatalyzed process ( $\Delta G_{\text{solv}}^\ddagger = 32.3$  kcal/mol, **TS-15** in Figure 1). These computed barriers suggest that this mechanism is unlikely. Moreover, the computed KIEs for this process (1.25 and 1.32, respectively) did not match the experimentally observed KIEs of  $\sim 1.85$  (eqs 5 and 6).

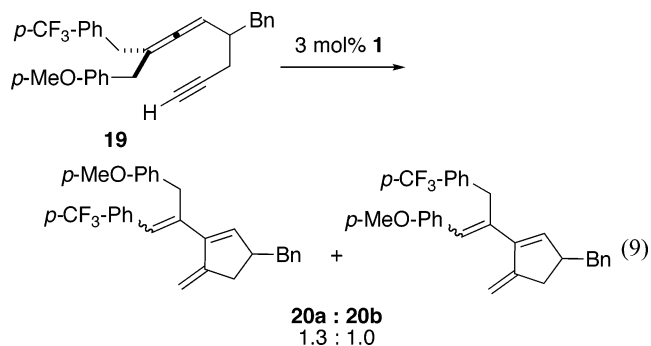
While the deuterium exchange experiments are consistent with in situ generation of phosphinegold acetylide (eq 3), independent evidence for acetylide participation in the catalytic cycle was sought. To this end, phosphinegold acetylide **2a'** was prepared by formation of the lithium acetylide of substrate **2a** and subsequent transmetalation with triphenylphosphinegold(I) chloride (eq 7).<sup>23</sup> However, as predicted from computations, the exposure of the acetylide **2a'** to reaction conditions

without added catalyst failed to furnish the desired products (eq 8).



**Mechanism via B or F: Metallacycles.** Despite extensive computational searching, no metallacycle intermediates similar to **B** or **F** could be found. Any attempts to locate these metallacycle intermediates computationally lead to substrate phosphinegold complexes with a preferential monoligation to either the alkyne or the allene (**17** and **18**, Figure 3). Indeed, this is not surprising, considering that, relative to other late transition metals, oxidative additions involving cationic phosphinegold(I) complexes are known to be difficult.<sup>24</sup>

A mechanism involving a metallacycle intermediate necessitates a  $\beta$ -hydride elimination step to generate product (Scheme 3). Such a reaction should be very sensitive to the electronic bias of the hydrogen being transferred. An experimental intramolecular Hammett study was designed to probe the nature of the hydrogen transfer. Cyclization of unsymmetric substrate **19** yielded a regioisomeric product distribution of 1.3:1.0,



(21) Figures prepared with CYLview: Legault, C. Y. *CYLview*, version 1.0b; UCLA: Los Angeles, CA, 2007.

(22) Computational study of copper-catalyzed pericyclic reactions has been reported: Himo, F.; Lovell, T.; Hilgraf, R.; Rostovtsev, V. V.; Noodleman, L.; Sharpless, K. B.; Fokin, V. V. *J. Am. Chem. Soc.* **2005**, *127*, 210.

(23) Schuster, O.; Liao, R.-Y.; Schier, A.; Schmidbaur, H. *Inorg. Chim. Acta* **2005**, *358*, 1429.

(24) Oxidative addition of phosphinegold(I)halide complexes to elemental halogens: Schneider, D.; Schier, A.; Schmidbaur, H. *Dalton Trans.* **2004**, 1995 and references therein.

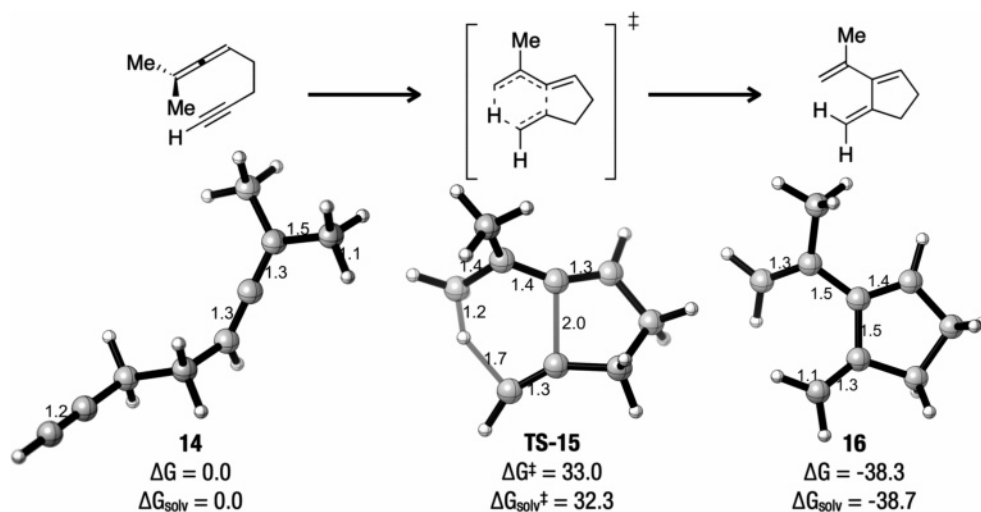


Figure 1. Uncatalyzed reaction: computed reactant, transition structure, and product.<sup>21</sup>

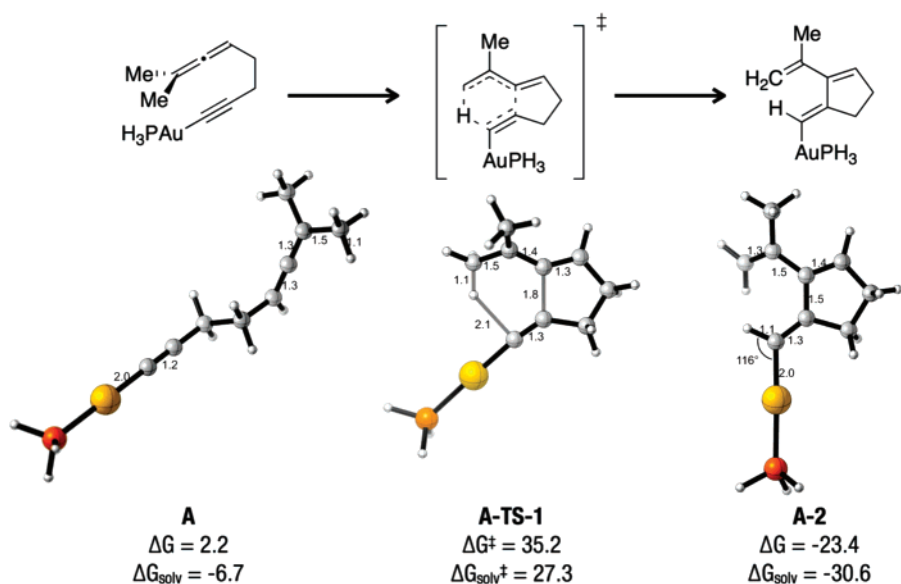


Figure 2. Computed reactant, transition structure, and product corresponding to the ene reaction of a gold acetylide **A**.<sup>21</sup>

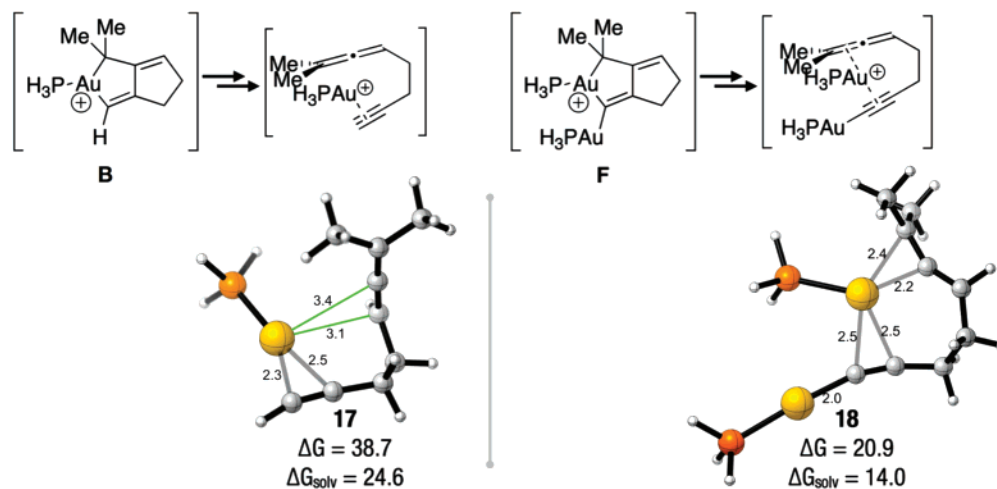
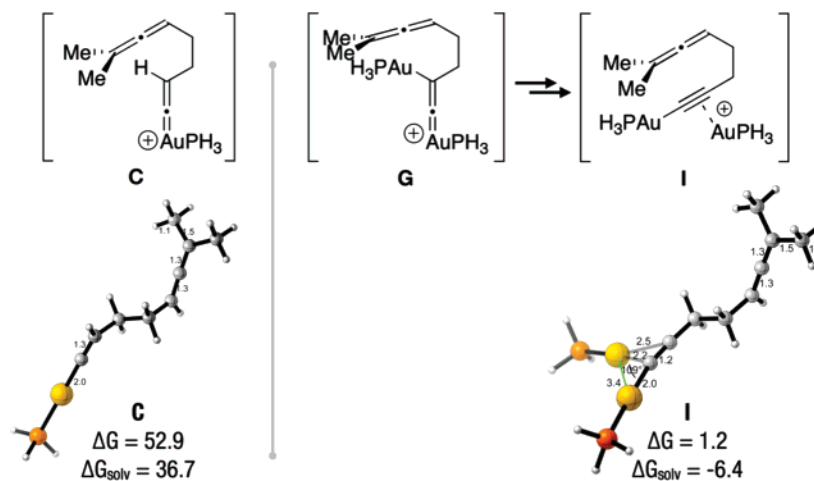


Figure 3. Computed intermediates, **17** and **18**, resulting from computational efforts to locate metallacycle intermediates **B** and **F**, respectively.<sup>21</sup>

slightly favoring transfer of the hydrogen benzylic to the *p*-trifluoromethyl group (eq 9). This near-equal distribution of isomers is suggestive of electronic neutrality in the hydrogen

transfer transition state and is inconsistent with a mechanism involving  $\beta$ -hydride elimination. Finally, the measured KIEs of  $\sim 1.85$  (eq 5 and 6) are inconsistent with transition metal-





**Figure 4.** Computed vinylidene intermediate **C** and the intermediate **I** arising from computational efforts to locate the gold acetylide vinylidene intermediate **G**.<sup>21</sup>

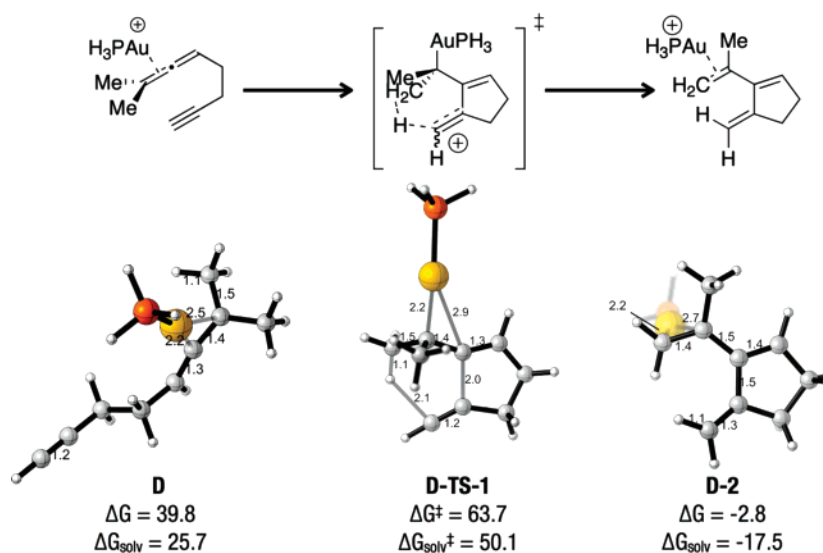
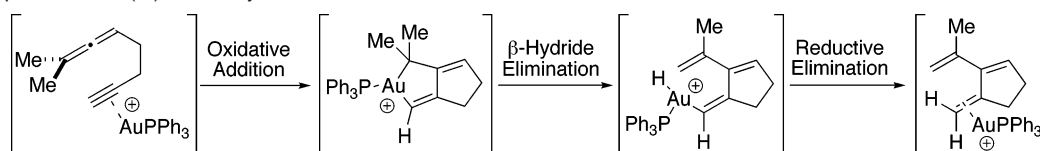


**Figure 5.** Computed intermediates and transition structures corresponding to the ene reaction of Au(I) phosphine allene coordination complex **D**.<sup>21</sup>

### Scheme 3. Hypothetical Au(III) Metallacycle Mechanism



catalyzed reactions that are proposed to proceed via metallacycle intermediates.<sup>25,26</sup>

**Mechanism via C or G: Gold Vinylidenes.** The gold vinylidene intermediate **C** was found to be extremely unstable ( $\Delta G = 52.9$  and  $\Delta G_{\text{solv}} = 36.7$  kcal/mol, Figure 4). Since this intermediate is higher in energy than the transition structure of the uncatalyzed reaction (Figure 1), a mechanism involving **C** is not operative. The gold vinylidene of the gold acetylide **G** is not a minimum, and calculations lead to spontaneously rearrangement to a structure corresponding to intermediate **I**.

**Mechanism via D or H: Catalysis by Phosphenegold Coordination to the Allene  $\pi$ -Bond.** The computed structures corresponding to the transformations arising from phosphenegold coordination to the allene of the substrate (**D**, Scheme 1) are shown in Figure 5.<sup>17</sup> This coordination mode leads to concerted C–C bond formation and asynchronous hydrogen transfer, similar to the uncatalyzed process. The free energy of activation for this process is prohibitively high ( $\Delta G^\ddagger = 63.7$  and  $\Delta G_{\text{solv}}^\ddagger = 50.1$  kcal/mol, **D-TS-1**), due to the development of an unstabilized vinyl cation in the transition state. In fact, the computed barrier is much greater ( $\Delta G_{\text{solv}}^\ddagger > 50$  kcal/mol) than that of the uncatalyzed reaction ( $\Delta G_{\text{solv}}^\ddagger = 32.3$  kcal/mol, **TS-15** in Figure 1).

The analogous computed structures corresponding to mechanism via **H** (Figure 6), which involves phosphenegold coor-

(25)  $[\text{Rh}(\text{CO})_2\text{Cl}]_2$  also catalyzes the same reaction, but the measured  $k_{\text{CD}_3}/k_{\text{CH}_3}$  isotope effect ( $1.19 \pm 0.05$ ) is much lower.

(26) Examples of  $k_{\text{H}}/k_{\text{D}}$  isotope effect on  $\beta$ -hydrogen elimination: (a) Ozawa, F.; Ito, T.; Yamamoto, A. *J. Am. Chem. Soc.* **1980**, *102*, 6457. (b) Evans, J.; Schwarts, J.; Urquhart, P. W. *J. Organomet. Chem.* **1974**, *81*, C37.

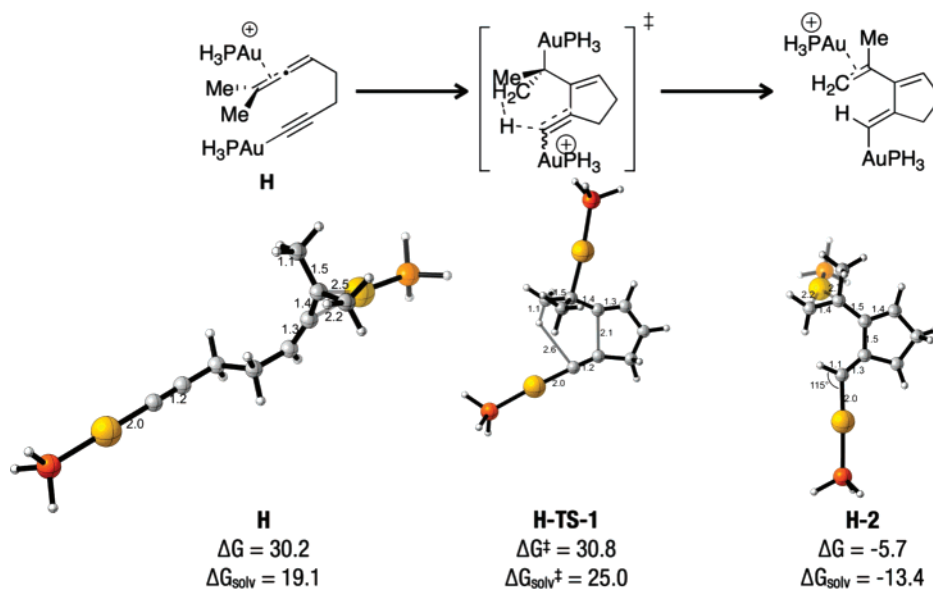


**Figure 6.** Computed intermediates and transition structures corresponding to the ene reaction of phosphinegold coordination to the allene of a gold acetylide, **H**.<sup>21</sup>

dination to the allene of a phosphinegold acetylide, closely resemble those involving **D** (Figure 5); it also features concerted C–C bond formation and asynchronous hydrogen transfer (**H-TS-1**). However, this process is much more facile because it does not incur the energetic penalty of transferring a single phosphinegold cation (**D** versus **H**, Scheme 1). This mechanism is still unlikely to occur because the free energy of activation ( $\Delta G_{\text{solv}}^\ddagger = 31.4$  kcal/mol, **H-TS-1**) is very similar to that of the uncatalyzed process ( $\Delta G_{\text{solv}}^\ddagger = 32.3$  kcal/mol, **TS-15** in Figure 1).

**Mechanism via E or I: Catalysis by Phosphinegold Coordination to the Alkyne  $\pi$ -Bond.** The cyclization involving phosphinegold alkyne complex **E** occurs via a stepwise process. C–C bond formation (**E-TS-1-syn** and **E-TS-1-anti**) following phosphinegold coordination leads to a relatively stable vinyl cation intermediate in which the gold is either syn or anti to the forming C–C bond (**E-2-syn** and **E-2-anti**, respectively). The subsequent hydrogen transfer (**E-TS-3-syn** and **E-TS-3-anti**) from an adjacent allenyl methyl group to the nascent allylgold furnishes the product phosphinegold complex **E-4**.<sup>27</sup>

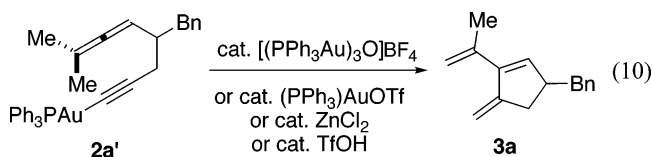
The anti coordination mode is favored over the syn for the C–C bond formation by  $\sim 7$  kcal/mol. Steric repulsions will cause the anti isomer to be even more strongly favored with larger alkylphosphine ligands. While subsequent hydrogen transfer is more favored for the syn than the anti isomer, isomerization of the vinyl gold intermediate **E-2** from the anti arrangement to the syn is extremely difficult ( $\Delta G^\ddagger = 44.4$  kcal/mol). The anti C–C bond formation (**E-TS-1-anti**) and subsequent hydrogen transfer process (**E-TS-3-anti**) exhibit free energy barriers of  $\sim 28$  kcal/mol. It is interesting to note that most of the barrier for C–C bond formation arises from the energetic penalty of transferring a single phosphinegold cation (**E** versus **I**, Scheme 1): **E-TS-1-anti** is essentially barrierless from **E**.

(27) Formation of a bicyclo[3.1.0]hexane intermediate has been proposed in previously reported gold-catalyzed cycloisomerization reactions of 1,5-enynes.<sup>5c</sup> The analogous intermediate is not accessible in the current reaction as it would require the formation of a strained bicyclo[3.1.0]hex-1-ene species, in violation of Bredt's rule.

The greater stability of the alkyne coordination pathway (**E** in Scheme 1) as compared to the allene coordination (**D** in Scheme 1 and **D-TS-1** in Figure 5) stems primarily from the stabilization of the developing allylic substituted cation versus a vinyl cation.

A mechanism involving intermediate **E** appears viable, although still relatively slow. We believe it does not actually occur for several reasons: (i) This mechanism fails to account for the inertness of nonterminal alkyne substrates.<sup>12</sup> (ii) Formation of the C–C bond is predicted to result in formation of a relatively stable vinyl gold intermediate (**E-2-anti**) that should be observable. Despite extensive trials to trap this intermediate via addition of methanol to the reaction mixture, products corresponding to this intermediate could not be isolated.<sup>6b</sup> (iii) Computed KIEs for this mechanism (1.02 and 4.04 for eqs 5 and 6, respectively) did not fit the experimentally observed KIEs of  $\sim 1.85$ .

Although the acetylide **2a'** was bench-top-stable in both solution and solid state, addition of trimer **1** afforded triene **3a** (eq 10). Use of  $\text{PPh}_3\text{AuOTf}$  also proved successful when applied toward the preformed acetylide **2a'**. Even simple Lewis acids such as  $\text{ZnCl}_2$  or Brønsted acid elicited product formation.<sup>28</sup>



As previously stated, the use of  $\text{PPh}_3\text{AuCl}/\text{AgOTf}$  leads to the formation of a complex mixture. In light of this, the cyclization of **2a'** by Brønsted acid catalysis shown in eq 10 is curious because this should amount to an equivalent process. However, complex **1** contains a basic oxo ligand that promotes deprotonation to form the gold acetylide (Scheme 2). Additionally, in the absence of formation of the phosphinegold acetylide,

(28) Reaction of analogous silver acetylides with various Lewis acids yielded no observable triene product.

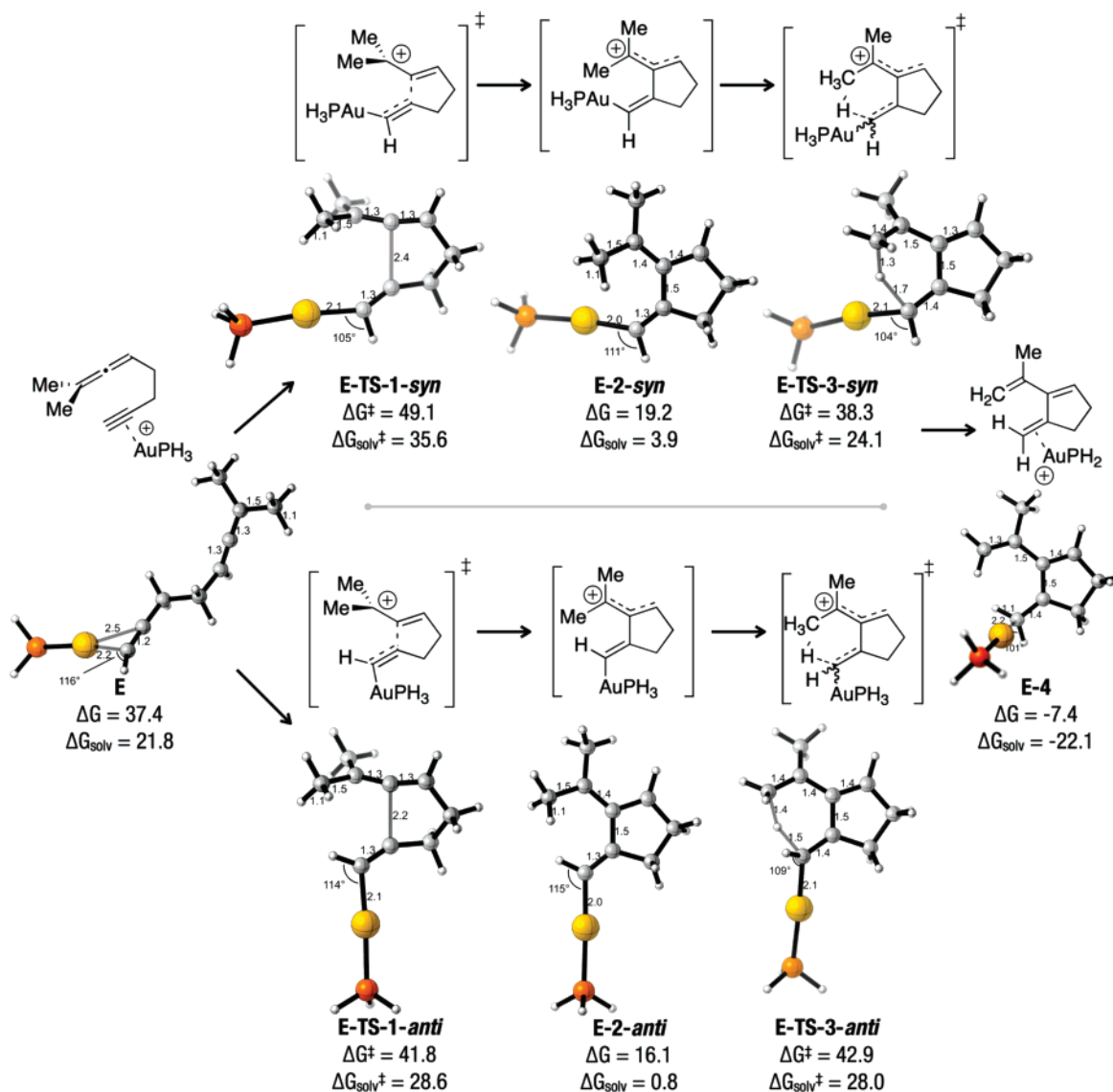
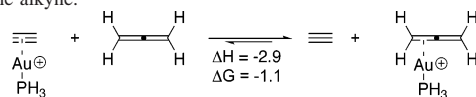


Figure 7. Computed intermediates and transition structures corresponding to the ene reaction of Au(I) phosphine alkyne coordination complex **E**.<sup>21</sup>

the phosphinegold cation may lead to an unselective reaction, perhaps due to pathways involving activation of the allene.<sup>29,30</sup> It is conceivable that phosphinegold could also catalyze the degradation of the allene in phosphinegold acetylide intermediate **D**, but we observe selective formation of the desired triene products. Additionally, while there is little difference in the preference for phosphinegold to coordinate to an alkyne or allene,<sup>30</sup> there is a strong preference ( $\sim 22$  kcal/mol) for coordination to an acetylide over an allene.<sup>31</sup>

(29) Examples of cycloisomerizations enallenes involving activation of allenes by cationic phosphine gold complexes: (a) Zhang, L. *J. Am. Chem. Soc.* **2005**, *127*, 16804. (b) Buzas, A.; Gagosz, F. *J. Am. Chem. Soc.* **2006**, *128*, 12614. (c) Lee, J. H.; Toste, F. D. *Angew. Chem., Int. Ed.* **2007**, *46*, 912. (d) Huang, X.; Zhang, L. *J. Am. Chem. Soc.* **2007**, *129*, 6398. (e) Luzung, M. R.; Mauleón, P.; Toste, F. D. *J. Am. Chem. Soc.* **2007**, *129*, 12402. (f) Lemiére, G.; Gandon, V.; Cariou, K.; Fukuyama, T.; Dhimane, A.-L.; Fensterbank, L.; Malacria, M. *Org. Lett.* **2007**, *9*, 2207. (g) Tarselli, M. A.; Chianese, A. R.; Lee, S. J.; Gagné, M. R. *Angew. Chem., Int. Ed.* **2007**, *46*, 6670.

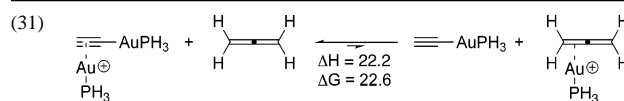
(30) There is a slight preference for the phosphinegold to coordinate to the allene over the alkyne.



The computed transformations following phosphinegold coordination to the alkyne of a phosphinegold acetylide (**I**, Scheme 1) are shown in Figure 8. This process is stepwise, similar to mechanism via **D** (Figure 7). C–C bond formation (**I-TS-1**) has a reasonable free energy barrier ( $\sim 21$  kcal/mol), leading to a *gem*-diaraalkene intermediate (**I-2**). The free energy barrier for the subsequent 1,5-sigmatropic hydrogen transfer (**I-TS-3**) is slightly lower ( $\sim 20$  kcal/mol). The reaction is exergonic by  $-45.5$  kcal/mol.

The structure of intermediate **I-4** requires some elaboration. The computed structure of this intermediate features a three-centered two-electron bond (Figure 9). The structure is best regarded as a vinyl anion coordinated by two phosphinegold cations.

The experimentally observed diastereoselective incorporation of hydrogen (eq 1) and anti incorporation of solvent deuterium (eq 4) are explained by the following: (i) the 1,5-sigmatropic





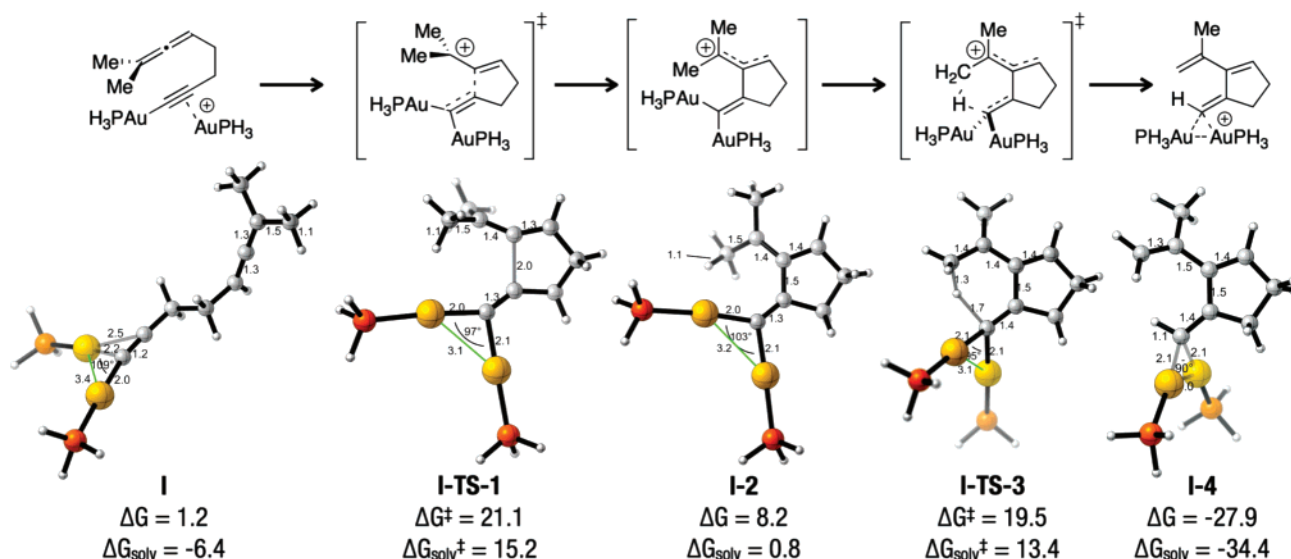


**Figure 8.** Computed intermediates and transition structures corresponding to the ene reaction of phosphinegold cation coordination to the alkyne of a phosphinegold acetylide, **I**.<sup>21</sup>

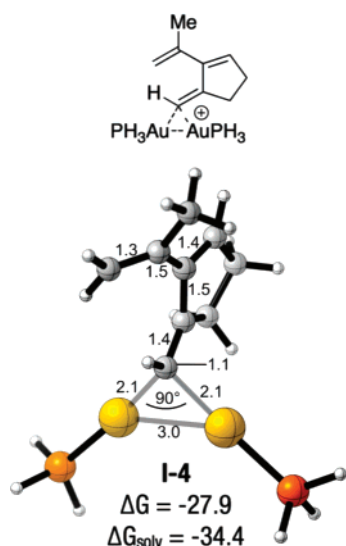


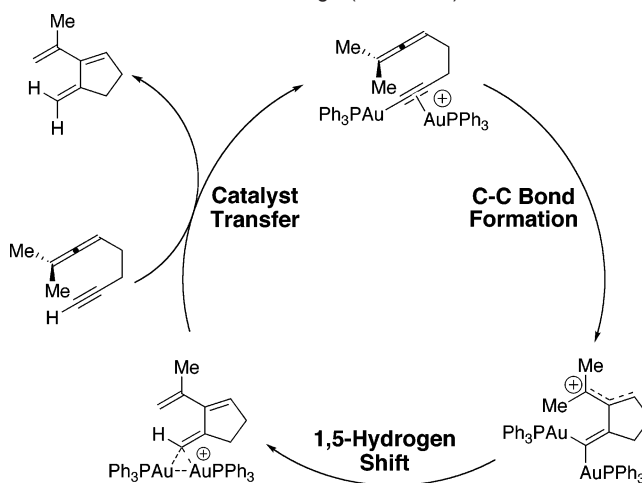
**Figure 9.** Side view of intermediate **I-4**.<sup>21</sup>

shift (**I-TS-3**) is stereospecific; (ii) subsequent isomerizations around the double bond of intermediate **I-4** are hindered by the steric bulk of the gold phosphines; and (iii) protodemetalations are known to occur stereospecifically.<sup>6c</sup> Additionally, the computed KIE values of mechanism **I** are 1.8 and 2.0, respectively, for eqs 5 and 6, which are in excellent agreement with experimentally observed KIE of  $\sim 1.85$  for both cases.<sup>32</sup>

The steady-state catalytic cycle of this reaction is summarized in Scheme 4. The coordination of a phosphinegold cation to the in situ generated phosphinegold acetylide lowers the alkyne lowest unoccupied molecular orbital (LUMO) toward 5-endo-dig cyclization, generating a *gem*-diaraalkene and tertiary allylic carbocation. A subsequent 1,5-hydrogen shift followed by protodemetalation and transfers of phosphinegold to another substrate closes the catalytic cycle (Scheme 4).

The free energy profile for the steady-state catalytic process via **I** is shown in Figure 10. The transfer of two phosphinegold

**Scheme 4.** Mechanism Involving **I** (Scheme 1)



cations from **I-4** to form species **I** and the release of product is exergonic by 10 kcal/mol. Efforts to trap the *gem*-diaraalkene **I-2** have failed, presumably because the subsequent hydrogen transfer is extremely fast ( $\Delta G_{\text{solv}}^{\ddagger} = 12.6$  kcal/mol) from this intermediate. The most difficult barrier of the catalytic cycle shown in Figure 10 is C–C bond formation step (**I-TS-1**) with an activation free energy of 21.6 kcal/mol. Unfortunately, the overall free energy barrier for the catalytic cycle cannot be computed because the transition structures of the phosphinegold acetylide formation could not be located in the gas phase and the actual barrier heights are dependent on the unknown instantaneous concentrations of every species in the reaction mixture. Regardless, the observation that the deuterium labels at the alkyne terminus tend to wash out in the product, while the starting material showed no comparable decrease, suggests that formation of the phosphinegold acetylide is an irreversible process and possibly rate-limiting (eq 11).

(32) This was the only case presented in this paper where the KIE was computed by use of a simple phosphine.

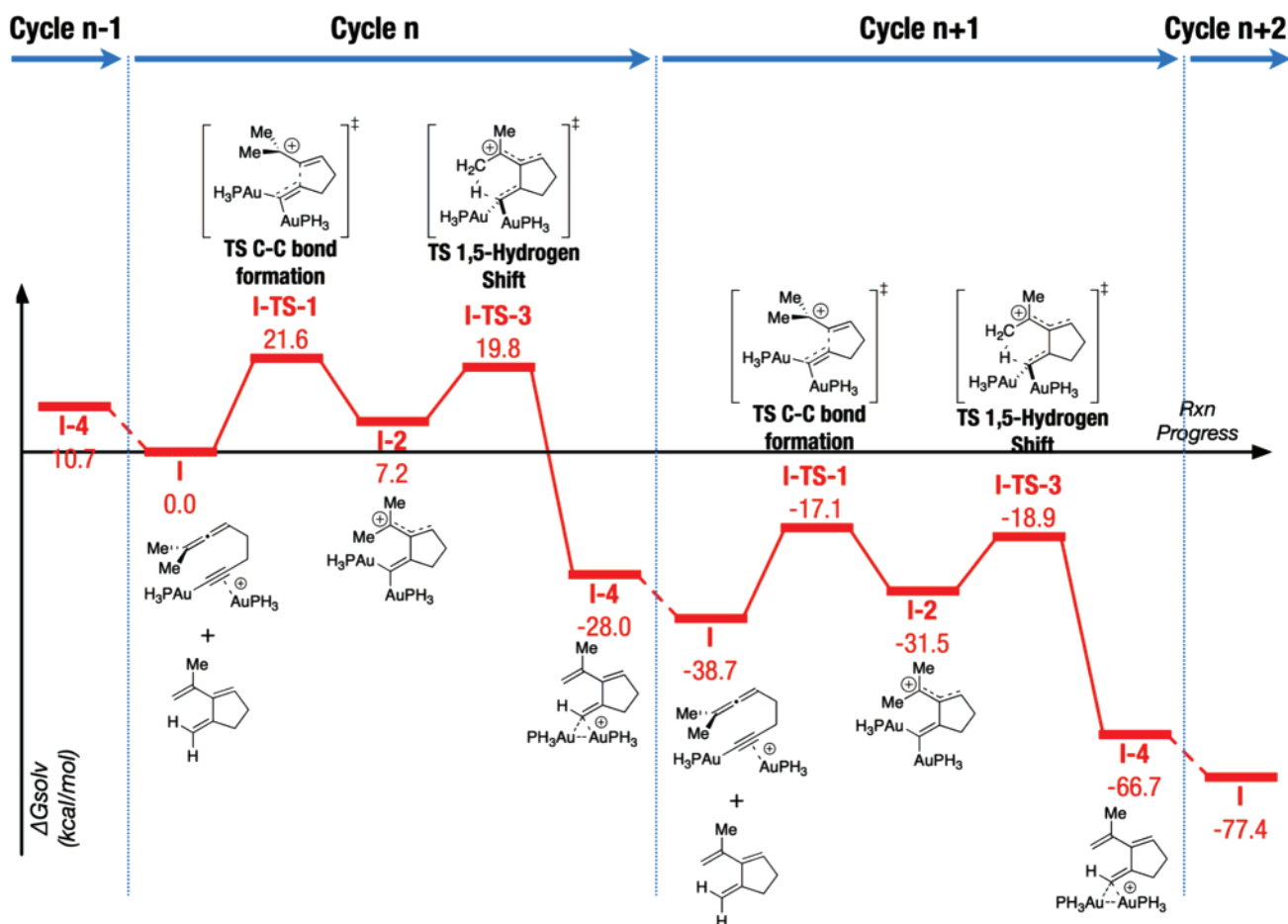
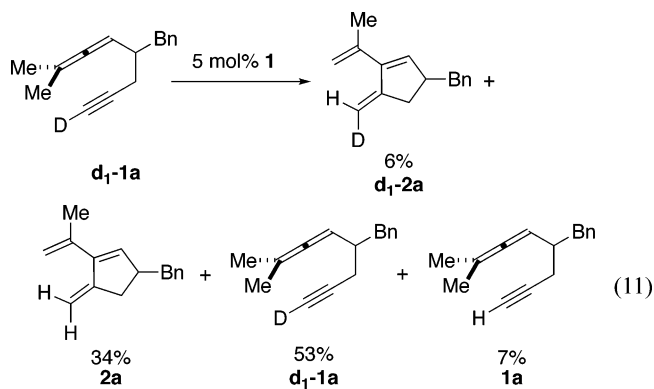


**Figure 10.** Free energy progress profile for two cycles in the mechanism via alkyne coordination to phosphinegold acetylide (I, Scheme 1). Free energies were computed by use of gas-phase standard state; dashed lines signify transfer of phosphinegold cations from products to reactants.



## Conclusions

In summary, we have presented a Au(I)-catalyzed rearrangement of allenyne to cross-conjugated trienes. Combined experimental and computational evidence reveal that a mechanism involving nucleophilic addition of an allene double bond to a phosphinegold-complexed phosphinegold acetylide is more likely than oxidative cyclization or simple nucleophilic addition to phosphinegold-complexed substrate.

**Acknowledgment.** F.D.T., P.M., and M.R.L. gratefully acknowledge the University of California, Berkeley, NIHGM (R01 GM073932), Merck Research Laboratories, Bristol-Myers Squibb, Amgen Inc., and Novartis for financial support. P.H.-Y.C. and K.N.H. gratefully acknowledge the University of California, Los Angeles, NIHGM (GM 36700), and NSF (CHE-0548209), for financial support. The computational study was facilitated through the Partnerships for Advanced Computational Infrastructure (PACI) through the support of the National Science Foundation. Computations were performed on the National Science Foundation Terascale Computing System at the SGI Altix Cobalt and the California Nano Systems Institute cluster. P.H.-Y.C. is grateful to Claude Y. Legault for helpful discussions.

**Supporting Information Available:** Experimental procedures and compound characterization data; Cartesian coordinates, energies, and thermodynamic corrections for all reported structures; complete ref 20. This material is available free of charge via the Internet at <http://pubs.acs.org>.

JA711058F